FAILURE CRITERIA FOR STAMPING ANALYSIS IN RADIOSS

Vincent Diviné[1*], Erwan Beauchesne[2], Qiang Zeng[2], Mircea Istrate[2], Subir Roy[3], Hariharasudhan Palaniswamy[3]

[1]Altair Development France, 5/10 rue de la Renaissance, 92184 Antony, FRANCE
[2]Altair Development France, 5/10 rue de la Renaissance, 92184 Antony, FRANCE
[3]Altair, 1820 East Big Beaver Road, Troy, MI 48083, USA

ABSTRACT: In this paper, several failure criteria are compared in their ability to predict necking point and failure propagation during a forming process. Strain based FLC criteria are widely used to evaluate feasibility of a component during a forming process and its usefulness is well known in the stamping industry. However, it has been shown that FLC criteria are strongly dependent on the strain-path history which makes it inaccurate for a multi-step simulation as well as for high strength materials. In addition, it remains mostly a post-processing tool so that failure mode is not taken into account during forming simulation. Hence, one purpose of this study is to demonstrate the benefit of an embedded failure criterion within the material law definition for forming process simulation. A couple of failure criteria available in RADIOSS®, a non-linear finite element based structural analysis solver, are compared and the feasibility of such approach as an industrial solution both in term of computation time and accuracy is demonstrated.

KEYWORDS: Failure criteria, Forming Limit Diagram, Stamping, Necking, RADIOSS®, Forming.

1 INTRODUCTION

Nowadays, numerical simulation plays a significant role in establishing the feasibility of manufacturing processes. It enables stamping specialists to iteratively improve the process by looking at defects such as wrinkling, necking or rupture, and springback without expensive tryouts. Wrinkling, necking and fracture can be detected through the commonly used post-processing tool Forming Limit Diagram (FLD). However, this diagram is based on the material-dependent Forming Limit Curve (FLC) determined from several special tests [1]. The purpose of this paper is to use a failure criteria embedded in the stamping simulation as an alternative to FLD method. The modeling has been done using HyperForm® and simulations have been performed using RADIOSS® [2] which are dedicated pre-processor and the explicit solver available in HyperWorks® software suit for stamping simulation. Standardized experimental processes used to determine FLD have been used for NUMISHEET'14 benchmark 1 (BM1) to predict the first necking location on a blank as well as the instance of its occurrence [3]. Using the BM1 report published in NUMISHEET'14 proceedings [4], the numerical model in this study is validated against experimental data and subsequently compared for several failure criteria. Initially FLD is used, as a post-processing tool where the predicted first onset necking point and non-linear strain paths

for certain points are considered to correlate with experimental data published in NUMISHEET'14 proceedings. Then, the same FLC is embedded in the numerical simulation, to show crack initialization at the exact location and time. Failure propagation is modeled first by setting stress level to zero once an element reaches the forming limit. Next, a more accurate approach using the extended finite element method (XFEM) [5] combined with FLD failure criterion is used. Finally, two other failure criteria available in RADIOSS are used and compared with results based on FLD criterion. Those are, the NXT criterion which can be approximated to a stress-based FLD [2], and the Modified Mohr Coulomb (MMC) failure criterion which calculates a damage value based on equivalent strain at fracture [2,6].

2 STAMPING PROCESS

NUMISHEET'14 BM1 considered three blank sizes (small, medium and full), three materials (Aluminium, DP600 and TRIP780 Steel), and two sets of tools (Shim1 and Shim4). The combination used in this paper is a full blank shape with DP600 steel and Shim4 tooling.

2.1 MODEL DESCRIPTION AND RESULTS

The stamping process consists of two stages. The first stage stamps the blank to obtain the drawbead

---

shapes around the blank periphery. The second one takes the blank to necking and fracture.

The following picture shows a cross-section through the tools and blank at the start of the second stage.
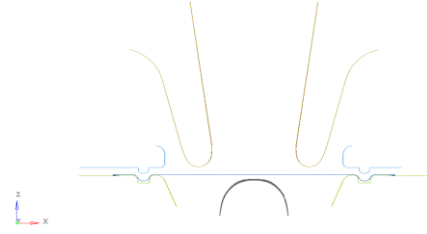

Fig. 1   *Fig. 1 Tools and blank initial position : Punch (brown), Blankholder (light-blue), Lower Tool (green), shim4 (black) and blank (dark-blue).*
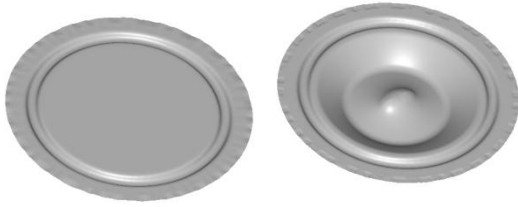

Fig. 2   *Blank shape at the end of first stage (left) and at the end of second stage (right)*

All material properties for DP600 steel used in this study have been taken from NUMISHEET'14 proceedings. A material law using an anisotropic Hill yield function along with an associated flow rule is used. The yield condition is show in Eq.1:

$$\phi(\sigma, \sigma_y) = \sigma_{Hill} - \sigma_y = 0 \qquad (1)$$

Where σ_{Hill} is the equivalent hill stress given as shown in Eq.2:

$$\sigma_{hill} = \sqrt{F\sigma_{yy}^2 + G\sigma_{xx}^2 + H\left(\sigma_{xx} - \sigma_{yy}\right)^2 + 2N\sigma_{xy}^2} \qquad (2)$$

Where F, G, H, N, are six Hill anisotropic parameters. In this study, a Swift law shown in Eq.3 is used to describe the hardening behaviour.

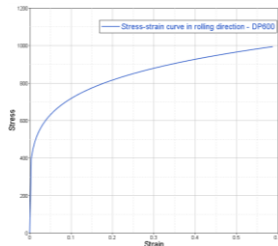$$\sigma_y = K(\varepsilon_0 + \varepsilon_p)^n \qquad (3)$$

Fig. 3   *Stress-strain curve in rolling direction for DP600 Steel*

2.2   STAMPING PROCESS VALIDATION

FLD criteria is used here as a post-processing tool. The lower punch force versus the lower punch displacement, from the time the blank touches the upper punch until fracture as shown in Fig.4, are the first results compared for validating the numerical model.
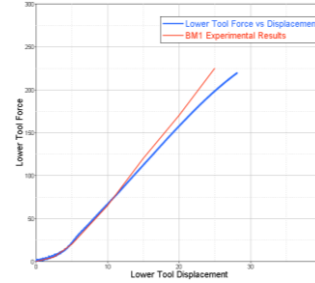

Fig. 4   *Lower tool force vs. displacement*

The non-linear strain paths of four specified points are then compared with experimental data (Fig.6). The first three points are localized on initial blank shape by coordinate system as shown in Fig.5 while the fourth one is the first to reach necking point on the blank upper surface as shown in Fig.7.
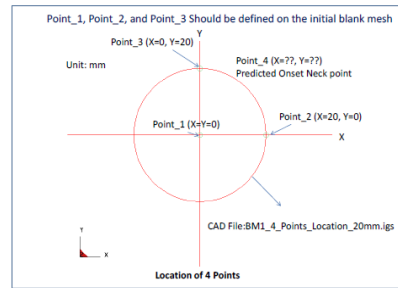

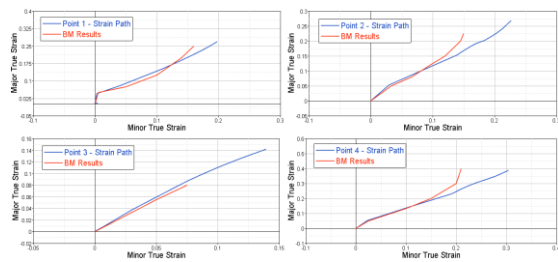**Fig. 5**   *Point locations on initial blank shape [6]*

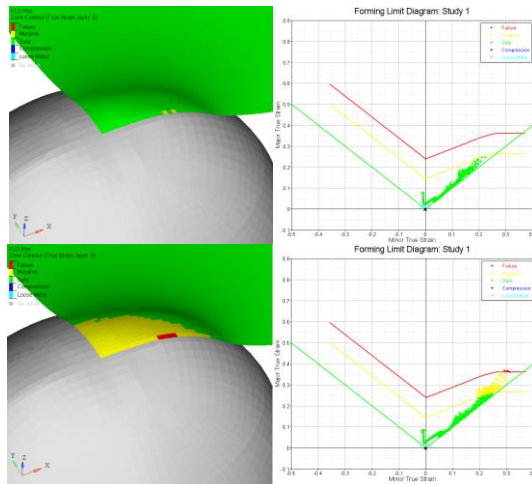**Fig. 6**   *Strain-paths of the four required points*

Fig. 7 *First point to reach necking (top) and failure (bottom).*

3 EMBEDDED FLD CRITERION

In the previous section, using FLD as post-processing requires an extra step to capture the exact time and location of the necking point by increasing the file output frequency to determine the exact time of necking and rupture. This inconvenience could be avoided by embedding FLD failure criterion in the numerical model itself. As soon an element reaches the FLC a failure model is then applied. Embedding failure criterion within simulation does not affect results until an element reaches input curves.

A first approach consists in using element deletion method when all integration points along the thickness of an element reach the limit. Stress level is set to zero for each integration point along thickness direction reaching FLC. As a result, the crack propagates through the blank as shown in Fig. 8.

Fig. 8 *Crack propagation with element deletion at forming limit*

Another approach used here to capture and propagate cracks in shell elements is the extended finite element method (XFEM), available in RADIOSS [2]. This new XFEM is based on phantom nodes methodology of Hansbo and Hansbo [10] and is used for the simulation of the propagating dynamic cracks without any need for re-meshing. This method, in conjunction with Level Set Method [11], permits arbitrary discontinuities to be modeled by finite elements without re-meshing. It also uses partition of unity [12] which adds enrichment functions to the displacement field within the element to take into account the local discontinuity.

The new XFEM formulation used for the modeling of cracks is particularly suited to explicit time integration methods. Although the crack shape inside an element has to be straight, its direction can change passing through the neighbor element making the path almost arbitrary. The crack propagation is handled as follows. When the strain at the crack tip reaches the fracture threshold (a smaller value for propagation than initiation), a strong discontinuity is injected (crack segment) ahead of the previous crack tip according to maximum hoop tensile stress. The crack pattern, shown in Fig.9, is much smoother than the crack opening obtained by the element deletion technique.

The first necking point is close to FLD based post-processing as well as, FLD embedded numerical simulation.
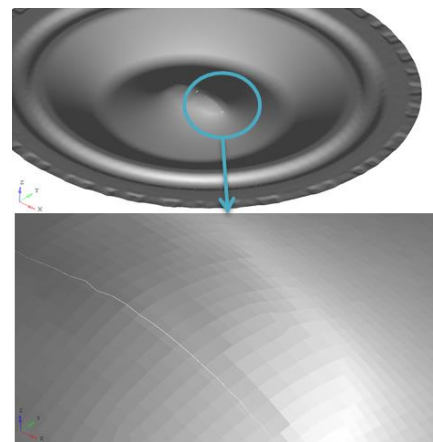

Fig. 9 *Crack propagation with XFEM approach*

As a conclusion, using a FLD failure criteria and a XFEM based crack propagation model embedded in stamping simulation captures the exact time and true fracture path which is useful to determine, for instance, whether the crack goes inside the trimming line and how it subsequently affects the formability.

4 COMPARISON WITH OTHER FAILURE CRITERIA

The previous approaches are all based on FLD criterion which requires the FLC. This information is not available all the time and a good alternative is to identify numerically this curve using an analytical failure criteria. We propose here to embed this analytical criterion in the simulation itself. Two such failure criteria NXT [2] and MMC (Modified Mohr Coulomb) [4] are already available in RADIOSS and illustrated in the following.

4.1 NXT FAILURE CRITERION

This criterion uses a stress level based FLD, as shown in Fig.10, built considering the localized

bifurcation as well as the instability theories for elastoplastic material. The forming limit diagram showed in the following picture is represented in the Sigma/h space, where Sigma is the in plane principal stress and h is the current work hardening modulus.
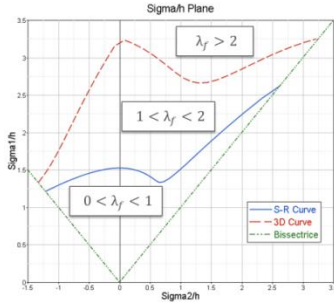

Fig. 10 *Forming limit diagram with NXT criterion*

Two limit curves are used as input, called SR and 3D curves. The SR curve represents the Stören-Rice's mode limit and the 3D curve represents the 3-dimensional localized mode limit. The lower SR curve defines start of necking, while the upper 3D curve defines fracture. Eventually, an instability factor is calculated as shown in Eq.4 in order to determine the failure zone:

$$\lambda_f = \frac{\sigma/h - (\sigma/h)_{SR}}{(\sigma/h)_{3D} - (\sigma/h)_{SR}} + 1 \qquad (4)$$

The value of λ_f defines the status of the fracture as follows:

Good   : $0 < \lambda_f < 1$
Warning: $1 < \lambda_f < 2$
Failed   : $\lambda_f = 2$.

Fig.11 shows the value of the instability factor of the blank at two different stages in the simulation.
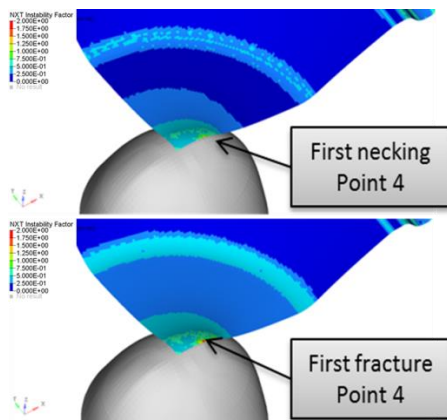

Fig. 11 *Evolution of NXT instability factor in a range [0,2]*

One can notice that the location of the first necking and failing point is equivalent to FLD failure criteria. Fig.12 shows stress-path of Point 4 on Sigma/h plane and the instability factor for the same location.
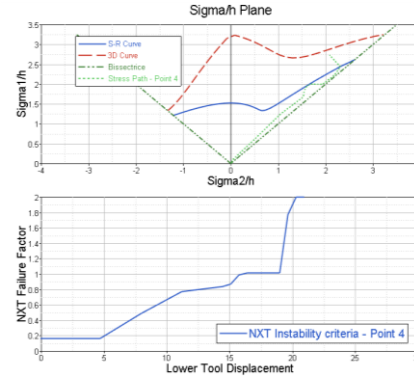

Fig. 12 *Stress path of Point 4 on Sigma/h plane (top), and variation of Instability Factor of Point 4 with lower tool displacement*

This failure criterion, being embedded in the solver, makes it possible to predict the first point to reach SR and 3D curves, and also the precise punch stroke when this happens. The possibility to input two curves enables the user to specify the necking and failure limits of the blank material.

4.2 MMC FAILURE CRITERION

As NXT failure criterion is based on a stress plane, it requires several experimental processes, equivalent to experiments needed for FLD evaluation. The MMC criterion is easy to use since it requires only three simple experimental tests to determine the three parameters for fracture mode.

Three experiments are necessary to determine the MMC parameters:

1) In plane shear test
2) Uni-axial tension test
3) Equi-biaxial tension test

Let C_1, C_2, C_3 be the three parameters for MMC fracture model. Damage accumulation is computed as:

$$D = \int_0^{\varepsilon_p} \frac{d\varepsilon_p}{\varepsilon_f(\theta,\eta)} \qquad (5)$$

Where ε_f the plastic strain fracture for the modified Mohr fracture criterion is given by:

$$\varepsilon_{\mathrm{f}} = \left\{ \frac{\sigma_y^0}{c_2} f_3 \left[\left(\sqrt{\frac{1+c_1^2}{3}} f_1 \right) + c_1 \left(\eta + \frac{f_2}{3} \right) \right] \right\}^{\frac{-1}{n}} \quad (6)$$

With

$$f_1 = \cos\left\{ \frac{1}{3} \arcsin\left[-\frac{27}{2} \eta \left(\eta^2 - \frac{1}{3} \right) \right] \right\}$$

$$f_2 = \sin\left\{ \frac{1}{3} \arcsin\left[-\frac{27}{2} \eta \left(\eta^2 - \frac{1}{3} \right) \right] \right\} \quad (7)$$

$$f_3 = c_3 + \frac{\sqrt{3}}{2-\sqrt{3}} (1-c_3) \left(\frac{1}{f_1} - 1 \right)$$

The fracture initiates at D=1.

Fig.13 shows a classic MMC fracture locus under plane stress condition.
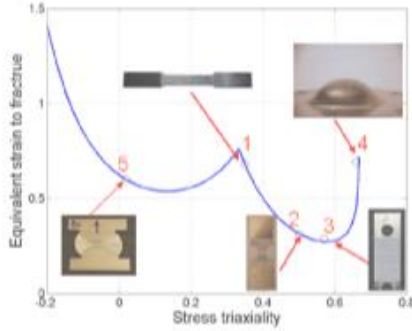

Fig. 13 *Typical MMC fracture locus [6]*

With this Modified Mohr Coulomb fracture model, the same location for the onset failure point shown by other criteria is found. Fig.14 shows the damage value of the blank just before failure.
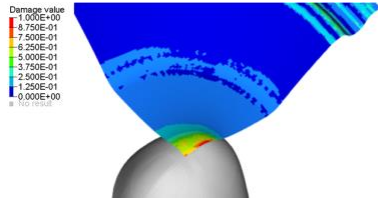

Fig. 14 *Damage value on blank before rupture, in a range [0,1]*

Fig. 15 *Crack propagation with MMC fracture model*

This fracture model can be evaluated through three simple experimental tensile tests and shows a good correlation with Forming Limit Diagram criterion.

5 COMPARISON

Crack propagation with a higher tool displacement can be first compared with all crack propagation approach based on FLC criterion and then with MMC and NXT failure criteria. The crack state at a 36.7mm displacement of the tool using respectively a FLD criterion (Fig.16) and a NXT or a MMC model (Fig.17) is shown below.

Fig. 16 *From left to right, crack propagation without and with XFEM method.*

Fig. 17 *From left to right, crack propagation using a MMC criterion and using a NXT criterion*

One can see that the overall shape of the crack pattern is similar for all cases and it is along the rolling direction. XFEM method predicts a larger crack as shown in Fig.17. This is due to a more accurate crack modelling capturing the physical behaviour based on stress direction. In case of MMC model, the damage is computed once per element, while FLD and NXT failure criteria are computed at each integration point through the thickness.

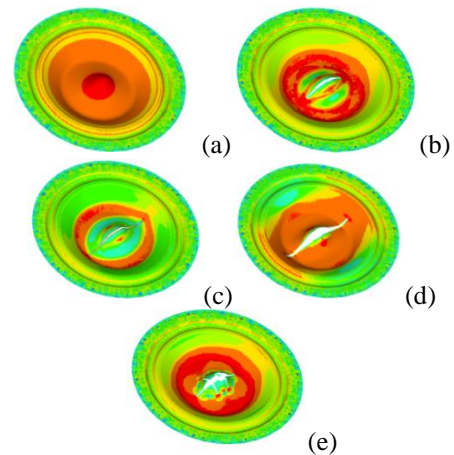(a)   (b)
(c)   (d)
(e)

Fig. 18 *Stress levels for different approaches, (a) No failure criteria, (b) Embedded FLD criterion with element deletion, (c) FLD criterion with XFEM, (d) MMC criterion, and (e) NXT criterion with element deletion.*

As shown in Fig.18, end stress level in principal direction shows a different distribution with and without an embedded facture model. This highlights the importance of embedding a failure criterion in the model for post-failure analysis like crack propagation, springback etc, instead of simply relying on the FLD as a post-processing tool.

Eventually, the time computation is not highly affected by the use of MMC or NXT facture model within the analysis in comparison with a simulation without any criterion and using FLD post-processing approach. The difference is about 10% for NXT model. However, XFEM method took about one third more time to compute.

6   CONCLUSIONS

The Forming Limit Diagram is currently the most commonly used tool to establish limits of forming process such as wrinkling, necking and failure. This tool can be used as a post-processing tool to observe failure points at the end of simulation, or the FLC can be embedded within numerical simulation, to track failure during the process. By embedding the FLC, the change of mechanical properties after necking and fracture point are taken into account during the stamping simulation. Other option such as the stress-based NXT failure criterion can be also be considered where two curves are used as input in order to evaluate necking and failure, depending on an instability factor. Finally, the Modified Mohr Coulomb is also effective in capturing the accumulated damage value. All these failure criteria can be modelled with RADIOSS, and combined with crack propagation model such as XFEM. This study shows that different failure criteria in RADIOSS give the same location of the necking and failure point and also correlates with experimental data in NUMISHEET'14 proceedings.

REFERENCES

[1]   British Standards (2008), ISO12004-2 - Metallic Materials - Sheet and Strip - Determination of Forming Limit Curves - Part 2: Determination of Forming Limit Curves in the Laboratory

[2]   RADIOSS 13.0 Documentation.

[3]   Benchmark 1 - Nonlinear strain path forming limit of a reverse draw: Part B: Physical try-out report Hongzhou Li, Jorge S. Cisneros, Xin Wu, Xu Chen, Xin Xie, Nan Xu and Lianxiang Yang AIP Conf. Proc. 1567, 27 (2013)

[4]   NUMISHEET 14' Proceedings.

[5]   A. Hansbo, P. Hansbo. *"A finite element method for the simulation of strong and weak discontinuities in solid mechanics"*, Computer methods in applied mechanics and engineering 2004, 193:3523–3540.

[6]   Dorel BANABIC, Liana PARIANU, Georges DRAGOS, Ioana BICHIS, Dan Sorin COMSA: *An improved version oft he modified maximum force criterion (MMFC) used for predicting the localized necking in sheet metals*. Proceedings of the romanian academy, Series A, Volume10, Number 3/2009, pp.000-000.

[7]   Xiaoming Chen, McMaster University : *Development of simulation technology for forming of advanced High Strengh Steel*. Open Access Dissertations and Theses. Paper 6841, 2012.

[8]   Yaning Li, Meng Luo, Jörg Gerlach, Tomasz Wierzbicki : *Prediction of shear-induced fracture in sheet metal forming.* Journal of Materials Processing Technology 210 (2010) 1858-1869.

[9]   Kirki Kofiani, Aida Nonn, Tomasz Wierzbicki, Christoph Kalwa and Carey Walters: *Experiments and Fracture Modeling of High-Strength Pipelines for High and Low Stress Triaxialities.* Proceedings of the Twenty-second (2012) International Offshore and Polar Engineering Conference.

[10]   Johnson G. R., Cook W. H.: *A constitutive model and data for metals subjected to large strains, high strain rates and high temperatures*. In: 7th International Symposium on Ballistics, 514-546, 1983

[11]   Stolarska M, Chopp DL, Moes N, Belytschko T, *"Modeling crack growth by level sets in the extended finite element method"*, International Journal for Numerical Methods in Engineering 2001; **51**(8):943–960.

[12]   I. Babuska, *"The partition of unity method"*, International journal for numerical methods in engineering 40 727–758 (1997).